Reactivity of [1,2-Benzisotellurazol-3(2*H*)-one] with Peroxynitrous Acid: Comparison with Ebselen Analogues

Djamaladdin G. Musaev*

Cherry L. Emerson Center for Scientific Computation, Emory University, Atlanta, Georgia 30322

Kimihiko Hirao

Department of Applied Chemistry, School of Engineering, The University of Tokyo, Tokyo 113-8656, Japan

Received: July 8, 2003; In Final Form: September 23, 2003

The mechanism of the reaction of [1,2-benzisotellurazol-3(2*H*)-one], ebtellur derivative **2__Te**, with peroxynitrous acid, HOONO, was elucidated at the density functional (B3LYP) level by using triple-ζ quality basis sets (BS1). It was found that in the gas phase the reaction, proceeding via the concerted pathway, occurs with $\Delta H = 0.3$ ($\Delta G = (3.4)$) kcal/mol HO−ONO bond cleavage barrier. The ΔG value of this barrier is only slightly larger than the (2.2) kcal/mol required for the HO−ONO bond homolysis. Inclusion of the solvent effects at the single-point PCM level increases the HO−ONO activation barrier to 5.8 kcal/mol. The product of the HO−ONO bond cleavage by **2__Te** is the complex **2__Te(OH)(ONO)**, which could decay via two distinct pathways leading to $NO_2^{\bullet}$ + **2__Te(OH)**$^{\bullet}$ and **2__Te(O)** + HONO. Both processes are endothermic in the gas phase: 23.7 (11.4) and 26.4 (14.5) kcal/mol, respectively. The inclusion of solvent effects makes the **2__Te(O)** + HONO formation more favorable in water. The comparison of the reaction of **2__M** + HOONO for M = Se and Te shows that the HO−ONO bond cleavage is fast for both metals, in the gas phase. However, the probability of competition in the concerted and stepwise pathways is higher for M = Te than for M = Se. The reaction of **2__Se** with HOONO produces only selenoxide **2__Se(O)**, while the reaction of **2__Te** with HOONO may produce the intermediate **2__Te(OH)(ONO)** and **2__Te(O)** + HONO. We also compared the mechanisms of the reactions of **2__Te** with $ONOO^-$ and HOONO.

I. Introduction

Peroxynitrite anion ($ONOO^-$, PN) and its protonated form, peroxynitrous acid (HOONO), have attracted great interest over the past several decades.[1−3] It has been demonstrated that peroxynitrite[4] and the radicals $^{\bullet}OH$ and $NO_2^{\bullet}$ formed upon homolysis of HO−ONO react rapidly with numerous biomolecules, and could be involve in many disease states.[5] Therefore, the search for drugs that can intercept this powerful oxidizing and nitrating agent and detoxify it becomes an important task.

One of the effective exogenous defense lines against PN toxicity is the glutathione peroxidase (GPx), a selenium-containing enzyme that destroys peroxides through their catalytic reduction by thiol glutathione (GSH).[6] This enzymatic process prompted us to test a variety of organo-selenium compounds against peroxynitrite,[7] among which ebselen (Chart 1) is the most promising.[8] The search for better selenium-containing antioxidants is continuing, and recently,[9] it was reported that allyl 3-hydroxypropyl selenide exhibits even better GPx activity than ebselen.

Simultaneously, the focus of experimental studies has extended to the organo-selenium analogues: organo-tellurium compounds. Some organo-tellurium compounds have been shown to exhibit potent antioxidative properties and higher GPx-like activity than their selenium analogues.[10−14] The observed different peroxynitrite reduction rates for organo-selenium and analogous organo-tellurium compounds suggests a basic difference between the reaction mechanisms of selenides and tellurides.[10] We believe that the elucidation of the differences and similarities of the organo-selenium and analogous organo-tellurium compounds is very important for designing better antioxidants against peroxynitrite.

CHART 1: Schematic Presentation of the Se and Te Compounds Used in This Work

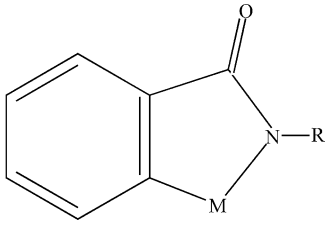

M= Se and R=Ph - **1, Ebselen**
M= Se and R=H - **2_Se**

M= Te and R=Ph - **1, Ebtellur**
M= Te and R=H - **2_Te**

In our previous papers we analyzed in detail the mechanisms of the reactions of ebselen (**1__Se**) and its numerous derivatives (see Chart 1) with PN[15] and HOONO,[16] as well as the mechanism of ebtellur derivative **2__Te** (see Chart 1) with PN.[17] This paper is a continuation of our previous studies, and elaborates on the mechanism of the reaction of **2__Te** with

10.1021/jp035969z CCC: $25.00
Published on Web 10/25/2003

HOONO. In addition, in this paper we compare the mechanism of the reaction

$$\mathbf{2\_\_Te} + \mathrm{HOONO} \quad (1)$$

with that for the reactions

$$\mathbf{2\_\_Se} + \mathrm{HOONO} \quad (2)$$

and

$$\mathbf{2\_\_Te} + \mathrm{ONOO^-} \quad (3)$$

reported earlier.[16,17] Similarities and differences of the reaction of **2__M** + $ONOO^-$ for M = Se and Te were analyzed in our recent paper[17] and will not be repeated here.

In general, the reaction of **2__M** with HOONO may occur via one- and/or two-electron oxidation pathways. The one-electron oxidation may proceed via either hydroxyl radical intermediate (possibly generated from HO−ONO homolysis) or the metastable reactive intermediate, ONOOH*.[18] Alternatively, the two-electron oxidation pathway involves O-atom transfer from peroxynitrite to **2__M** to form the corresponding oxides. Thus, peroxynitrite reactions with organic and inorganic species are certainly more complex than simple "oxygen atom" transfer, and the elucidation of their mechanisms requires more comprehensive (both experimental and theoretical) studies.

Furthermore, a majority of the reactions involving peroxynitrite take place in hydrophobic environments or in aqueous solution with a high content of organic material, at lipid/water or on gas/liquid interfaces, and, in general, are solvent dependent. Therefore, elucidation of the role of solvent effects on the mechanism of the reaction of **2__Te** with peroxynitrite is very important. In the present paper we include the solvent effects in the calculations using the single-point Polarizable Continuum Model[19] approach.

Previously, several theoretical studies on the reaction of the peroxynitrite with various organic and inorganic molecules have been reported.[20−22] The B3LYP/6-31G* calculations of Houk and co-workers[20d] have demonstrated the existence of the hydrogen-bonded [$HO^{\bullet}\cdots NO_2^{\bullet}$] radical pair, which is predicted to be involved in the peroxynitrite-to-nitrate isomerization and one-electron oxidation processes. However, the recent studies of Musaev and Hirao,[16] using higher level methods (such as MP2 and CCSD(T)), and including entropy and explicit solvent effects in the calculations, did not support the existence of this radical pair. Shustov and co-workers[22] applied computational methods to study the mechanism of aliphatic C−H bond oxidation in methane, propane, isobutane, propene, and 1,4-pentadiene with peroxynitrous acid and peroxynitrite anion. They analyzed three different mechanisms, namely, (a) direct oxygen insertion into the C−H bond (two-electron oxidation), (b) H-atom abstraction (one-electron oxidation), and (c) HO−ONO bond homolysis to form the hydroxyl radical. Their data included entropy effects and supports the mechanism c, an involvement of discrete hydroxyl radicals in lipid peroxidation by O_2 initiated in the presence of peroxynitrite. Musaev and co-workers[15,16] arrived at similar conclusions on the mechanisms of the reaction of ebselen (and its derivatives) with peroxynitrite using the B3LYP/6-311+G(d,p) approach. These calculations demonstrated that, at the enthalpy level, the two-electron oxidation of ebselen (and its derivatives) is energetically the most favorable pathway both in the gas phase and in solution. However, the inclusion of entropy corrections makes the one-electron oxidation pathway the most favorable in the gas phase.

TABLE 1: B3LYP/BS1 Calculated Relative Energies (in kcal/mol) of All Structures Reported Here

	gas phase				
structures	ΔE_{tot}	ΔE_{tot} + ZPC	ΔH	ΔG	water
2_Te + *cis*-HOONO	0.0	0.0	0.0	0.0	0.0
2_Te(HOONO)_with_OH	−7.6	−7.1	−6.4	1.7	
2_Te(HOONO)_with_N	−5.9	−5.3	−4.5	3.1	
2_Te(HOONO)_with_H	−5.3	−5.0	−5.2	6.1	
2_Te-TS1(O−O activ.)	−6.8	−6.9	−6.1	3.4	5.8
2_Te(OH)(NO_2)	−52.4	−50.9	−50.8	−38.5	−45.0
2_Te(O)(HONO)	−36.0	−35.2	−35.2	−24.8	
2_Te(OH) + NO_2	−26.8	−275	−27.1	−27.1	−18.2
2_Te(O) + HONO	−24.5	−24.5	−24.4	−24.0	−27.5

Recently, Musaev and co-workers[23] reported the B3LYP/6-311+G(d,p) studies of the mechanisms of the reactions of dimethyl sulfide (DMS) and dimethylselenide (DMSe) with peroxynitrite anion, $ONOO^-$, and peroxinitrous acid, HOONO. They found that the gas-phase reactions with $ONOO^-$ proceed via an O-atom transfer mechanism and produce the corresponding oxides (DMSO and DMSeO, respectively) and NO_2^- anion. The rate-determining barrier, the O−O bond cleavage, is found to be higher by 6−7 kcal/mol for DMS than for DMSe, indicating that DMSe is more reactive toward $ONOO^-$ than DMS. The inclusion of solvent effects decreases the rate-determining barrier and makes it less than 13.5 kcal/mol in aqueous solution for the DMS reaction. The reaction of DMS with *cis*-HOONO might proceed via two distinct pathways, stepwise (starting with homolysis of the HO−ONO bond to discrete $HO^{\bullet}$ and $ONO^{\bullet}$ radicals) and concerted (proceeding via an O−O bond cleavage transition state), and is much faster than that with $ONOO^-$. It is predicted that the reaction of DMS with HOONO in the gas phase most likely proceeds via the stepwise pathway only after including entropy effects. However, in the solution phase the stepwise and concerted pathways will effectively compete with each other.

II. Calculation Procedures

All calculations were performed with the quantum chemical package GAUSSIAN-98.[24] The geometries, vibrational frequencies, and energetics of all structures were calculated by using the hybrid density functional theory, B3LYP.[25] In these calculations, we used the 6-311+G(d,p) split-valence basis sets for all atoms except Te. For Te, we used the Stuttgart−Dresden relativistic effective core potential and associated basis set.[26] The combination of these basis sets will be called BS1. Previously, we have demonstrated that the B3LYP/BS1 approach provides very good agreement with experimental values for the optimized geometries of the numerous Te-containing species.[17] In this paper we extended the calibration of the methods used and the basis sets for the various compounds of S, Se, and Te. Data presented in Table 1S of the Supporting Information show that the increase of basis sets of O, S, and Se from 6-311+G(d,p) to 6-311+G(3df,p) slightly improves the agreement between the calculated and experimental[27] values of M−M and M−O bond distances for M = S and Se. Further improvement of the basis set to the aug-cc-pvqz set for S and O has an insignificant effect on the calculated bond distances. The BS1 basis set used for Te compounds provides slightly less accurate bond distances for Te_2 and TeO molecules compare to their S and Se analogues.

However, the M−M and M−O binding energies calculated at the B3LYP/BS1 level for M = S, Se, and Te are in equally

reasonable agreement with their experimental[27] values: the difference between their calculated ΔH and experimental values is within 5−10 kcal/mol (see Table 2S of the Supporting Information). The increase of basis sets from 6-311+G(d,p) to 6-311+G(3df,p) for O, S, and Se only slightly improves this agreement: the ΔH values of the S−S, Se−Se, S−O, and Se−O binding energies calculated at the B3LYP/6-311+G(3df,p) level are −1.3, 8.7, -1 ± 2.3, and 4.4 ± 5.1 kcal/mol different from their experiment values, respectively. Again, further improvement of the basis set to the aug-cc-pvqz for S and O has an insignificant effect on the calculated bonding energies. Thus, these data clearly demonstrate that the B3LYP/BS1 approach used in this paper provides reasonably accurate results for both the geometry and energy of the S, Se, and Te compounds, while to obtain the most accurate results it is necessary to use the more expensive B3LYP/6-311+G(3df,p) approach.

Previously,[28] it was shown that the B3LYP/6-311+G(d,p) approach provides excellent geometries compared with the more sophisticated approaches, such as CCSD(T), G2, and CBS-Q, using the 6-311+G(d,p) basis sets. However, we[16] and others[21,29] have demonstrated that the B3LYP/6-311+G(d,p) approach underestimates the calculated energetic barriers by about 5 kcal/mol compared to the CCSD(T) and QCISD(T) methods. In the current paper we discuss relative energies calculated at the same level of theory, therefore, we believe that any underestimation of the calculated barriers by the B3LYP method will not affect our general conclusions.

The solvent effect on the mechanism of reaction 1 was examined at the Polarizable Continuum Model[19] level with use of the BS1 basis set and the B3LYP/BS1 optimized geometries, referred to below as PCM-B3LYP/BS1. In these calculations we used water as the solvents, the default dielectric constant of which was taken from the Gaussian-98 program. In the literature[30] it was shown that PCM solvation effects are less dependent on the basis set and on the calculation level.

Note that the thermodynamic analyses were carried out for a temperature of 278.15 K and 1 atm of pressure, using the principal isotope for each element type and un-scaled vibrational frequencies (all these conditions are defaults in the Gaussian 98 quantum chemical package that was used in these calculations).

This paper is organized as follows. In Section III.1, we discuss the mechanism of the reaction of **2__Te** + HOONO in the gas phase and in water. We compare the potential energy surfaces (PESs) of the reactions of **2__Te** and **2__Se** with HOONO, as well as the reactions of **2__Te** with PN and HOONO, in Sections III.2 and III.3, respectively. In the final section, Section IV, we draw conclusions from these studies.

Note that the peroxynitrite anion ($ONOO^-$), peroxynitrous acid (HOONO), as well as the possible nitrogen-containing products of the reaction of **2__Te** with HOONO and PN, and the molecules NO_2, NO_2^-, NO_3^-, and HONO have been the subject of numerous studies.[31] Therefore, here we will not discuss those molecules, while we include their calculated geometries and energetics in Tables 3S and 4S of the Supporting Information. Here, we would like to point out that the previous studies[32] of peroxynitrous acid, HOONO, have shown that the cis-perp and cis-cis isomers of this molecule are energetically the lowest ones, and are practically degenerate in energy and can easily rearrange to each other. Therefore, we study the reaction of **2__Te** with the only cis-cis isomer of HOONO (for simplicity, below we refer to *cis-cis*-HOONO as "*cis*-HOONO", see Figure 1).

III. Results and Discussions

III.1. The Mechanism of the Reaction of 2__Te with HOONO in the Gas Phase. In general, the reaction of **2__Te** with HOONO, reaction 1, may proceed via two pathways: stepwise and concerted. The calculated important geometrical parameters of the intermediates, transition states, and products of reaction 1 are shown in Figure 1. Their relative energies are presented in Table 1.

We first address the concerted pathway, which starts with coordination of *cis*-HOONO to reactant **2__Te**. The resulted molecular complex **2__Te(HOONO)** may have numerous isomers. In this paper we isolated only three of them: **2__Te(HOONO)__with__OH**, **2__Te(HOONO)__with__H**, and **2__Te(HOONO)__with__N**. Among these isomers, the **2__Te(HOONO)__with__OH**, where *cis*-HOONO is coordinated to **2-Te** via its OH-end, is slightly more favorable: it is 6.4 kcal/mol stable relative to the dissociation limit **2__Te** + ***cis*-HOONO** at the ΔH level, while at the Gibbs free energy level (ΔG) it is unstable by (1.7) kcal/mol (in this paper, we present the ΔH and ΔG values without and with parenthesis, respectively). Below we elucidate only the reaction mechanism corresponding to the OH-end coordination of *cis*-HOONO to **2-Te**. The other possible coordination modes of *cis*-HOONO to **2-Te** are expected not to make significant contributions to the mechanism of reaction 1.

At the next step of the reaction the HO^3-O^2 bond cleavage occurs at the **TS1(O−O activ.)** transition state, which is confirmed to be a real transition state with one imaginary frequency of $299i$ cm^{-1}. In **TS1** the broken HO^3-O^2 bond is elongated by 0.136 Å, and the $N-O^2$ bond (π-bond) that is formed is shortened by 0.071 Å, relative to their values in the pre-reaction **2__Te(HOONO)** complex. The nascent $Te-O^3H$ bond has a distance of 2.657 Å. The ΔH value of the HO^3-O^2 bond cleavage barrier is calculated to be 0.3 kcal/mol relative to the pre-reaction complex **2__Te(HOONO)**. As seen in Table 1, the inclusion of the entropy corrections destabilizes the pre-reaction complex **2__Te(HOONO)** and **TS1**. Therefore, the ΔG value of the HO^3-O^2 bond cleavage barrier should be calculated from the reactants, **2__Te** + HOONO, and is found to be (3.4) kcal/mol.

Intrinsic reaction coordinate (IRC)[33] calculations show that the product of the O^3-O^2 bond cleavage is the complex **2__Te(OH)(ONO)**, which lies 50.8 (38.5) kcal/mol lower than reactants, **2__Te** + *cis*-HOONO. The **2__Te(OH)(ONO)** product could decay via two distinct pathways. The first one, called the dissociative or "radical" pathway, leads to $NO_2^\bullet$ and **2__Te(OH)$^\bullet$** radicals, and is endothermic by 24.7 (11.4) kcal/mol. Note that the dissociation of **2__Te(OH)(NO_2)** to $HO^\bullet$ and **2__Te($NO_2^\bullet$)** is expected to be slightly less favorable and will not be discussed.

The second process starting from the same **2__Te(OH)(NO_2)** complex is the H-atom transfer pathway. It proceeds via the H-atom transfer from the OH to the ONO fragment and leads to the **2__Te(O)(*cis*-HONO)** complex, which is confirmed to be a real minima with all positive frequencies. The reaction **2__Te(OH)(NO_2)** → **2__Te(O)(*cis*-HONO)** is endothermic by 15.6 (13.7) kcal/mol. All our attempts to locate a transition state (**2__Te-TS2(H-transfer)**) connecting **2__Te(OH)(NO_2)** with **2__Te(O)(*cis*-HONO)** failed and led either to the reactant complex **2__Te(OH)(NO_2)** or to the product complex **2__Te(O)(*cis*-HONO)**. These calculations indicate that the H-atom transfer barrier calculated from the complex **2__Te(O)(*cis*-HONO)** is very small because of the high exothermicity of the reaction **2__Te(O)(*cis*-HONO)** →

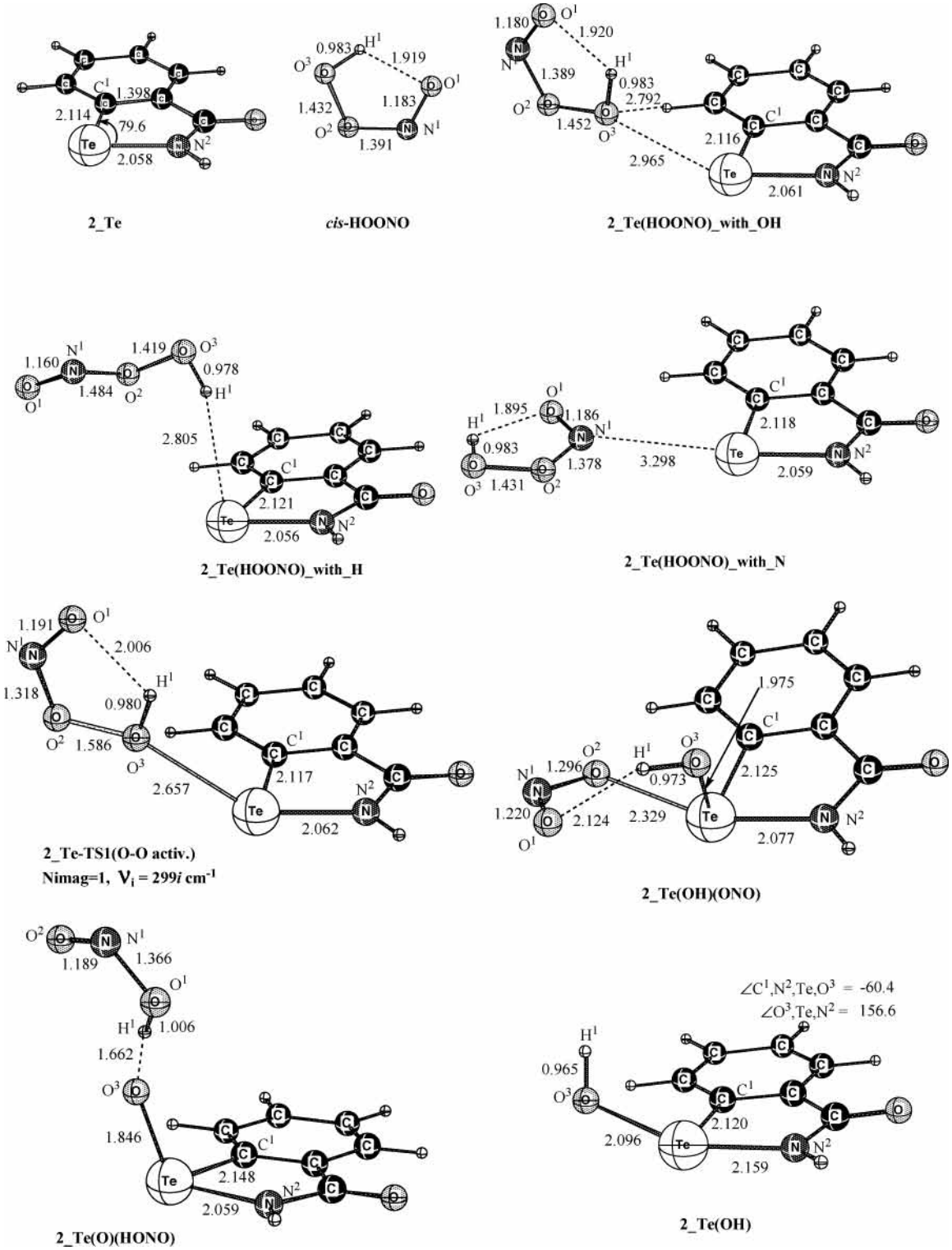

Figure 1. Calculated important geometries (distances in Å, angles in deg) of the reactants, intermediates, transition states, and possible products of the reaction of **2__Te** with HOONO.

2__Te(OH)(NO$_2$). The dissociation of HONO from the complex **2__Te(O)(*cis*-HONO)** is a very easy process and occurs with 10.8 (0.8) kcal/mol energy loss.

Comparison of these two processes, which start from the complex **2__Te(OH)(NO$_2$)**, shows that both of them are endothermic: 23.7 (11.4) and 26.4 (14.5) kcal/mol for the **2__Te(OH)**$^\bullet$ + NO$_2^\bullet$ and **2__TeO** + HONO dissociation limits, respectively. Thus, in the gas phase, one may expect the final product of the reaction **2__Te** + HOONO to be the complex **2__Te(OH)(NO$_2$)**, which can later dissociate either to **2__Te(OH)**$^\bullet$ and NO$_2^\bullet$ radicals or to **2__TeO** and HONO molecules. NO$_2$ dissociation occurs with slightly, 2.7 (2.9) kcal/mol, less energy loss than the dissociation of HONO.

The first step of the alternative, stepwise, pathway is the HO−ONO homolysis to yield the radicals HO$^\bullet$ and NO$_2^\bullet$. This homolysis proceeds with an energy of 12.3 (2.2) kcal/mol in the gas phase, according to the B3LYP/6-311+G(d,p) calculations. The B3LYP method with the larger basis sets, 6-311+G(3df,p), makes it 14.7 (3.9) kcal/mol. The previous calculations at the various levels of theory predicted an enthalpy

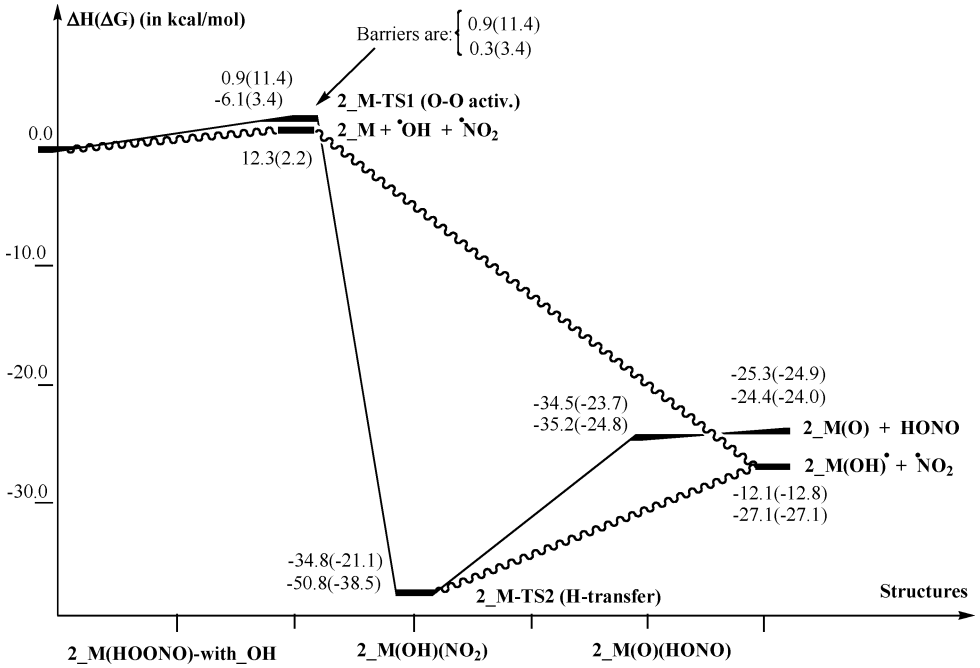

Figure 2. Schematic representation (based on Δ*G* values) of potential energy surfaces of the reaction **2__M** + HOONO, for M = Se (the first line) and Te (the second line), calculated at the B3LYP/6-311+G(d,p) and B3LYP/BS1 levels, respectively. Here, we have presented energies of only the lowest possible isomers of calculated intermediates and transition states. The numbers outside the parentheses are Δ*H* values, while those inside the parentheses are Δ*G* values.

of 20−22 kcal/mol[20d,34] for HO−ONO homolysis in the gas phase. Recently, Janoschek and co-workers[35] reported Δ*H* and Δ*G* values of 18.6 and (8.3) kcal/mol for HO−ONO homolysis in the gas phase using the more sophisticated G3MP2B3 method. The experimentally reported[36] enthalpy and Gibbs free energy of HO−ONO homolysis are 21 ± 3 and 11 ± 3 kcal/mol in the gas phase and 18 ± 1 and 17 ± 1 kcal/mol in water, respectively. These data clearly show that (a) the entropy effect is significantly smaller in water than in the gas phase and (b) the B3LYP/6-311+G(d,p) approach used in this paper underestimates the HO−ONO homolysis by 6−7 kcal/mol and should be used with great care.

In the next step, the HO• and NO_2• radicals coordinate to the **2__Te** complex step-by-step and/or simultaneously to form the **2__Te(OH)•**, **2__Te(NO_2)•**, and **2__Te(OH)(NO_2)** products, respectively. Our calculations show that HO• coordinates to **2__Te** a few kilocalories/mole more strongly than NO_2• does. Therefore, below we will not discuss the structure and energetics of the less stable **2__Te(NO_2)** complex. The **2__Te(OH)•** complex, the structure of which is given in Figure 1, is 39.4 (29.3) kcal/mol stable relative to the dissociation limit of **2__Te** + HO•.

The overall potential energy surface of the reaction of **2__Te** with *cis*-HOONO consists of both the concerted and stepwise pathways and is shown in Figure 2 (for simplicity this figure does not include the weakly bound pre-reaction complex **2__Te(HOONO)** and the **H-transfer** transition state).

The comparison of the data given in Figure 2 shows that, at the Δ*H* level, in the gas phase, reaction 1 proceeds via the concerted pathway with only a 0.3-kcal/mol barrier, calculated from the pre-reaction complex **2__Te(HOONO)**. However, the inclusion of entropy corrections (Δ*G* values) makes the concerted O−O bond cleavage barrier (3.4) kcal/mol, which is larger than the (2.2) kcal/mol required for HO−ONO bond homolysis. Therefore, one may expect that at the Δ*G* level the stepwise pathway to be more favorable than (or comparable to) the concerted one. As pointed out above, the B3LYP/6-311+G(d,p) and B3LYP/BS1 approaches used in this paper underestimate both the concerted O−O bond cleavage barrier and the HO−ONO bond homolysis. However, the values of these underestimations are shown to be similar (5−7 kcal/mol), and therefore unlikely to affect the conclusion above.

Inclusion of the solvent effects at the single-point PCM[19] level (PCM calculations provide the value called Δ*G*(solution), which does not include zero-point energy and entropy corrections, and should be compared only with the Δ*E* value for the gas phase) destabilizes the **2__Te(HOONO)** complex and the **TS1 (O−O activ.)** transition state relative to the reactants, and slightly increases the O−O activation barrier to 5.8 kcal/mol.

Furthermore, the solvent effects change the dissociation energy of **2__Te(OH)(NO_2)** to radicals NO_2• and **2__Te(OH)•** only slightly: from 25.6 kcal/mol in the gas phase to 26.8 kcal/mol in water. However, they significantly reduce the **2__Te(OH)(NO_2)** to **2__Te(O)** + HONO dissociation energy: from 27.9 kcal/mol in the gas phase to 17.5 kcal/mol in water. As a result, the H-atom transfer pathway becomes more favorable in water. The reported 17.5 kcal/mol dissociation energy of the **2__Te(OH)(NO_2)** → **2__Te(O)** + HONO reaction does not include entropy and temperature corrections, which are estimated to be 11.4 kcal/mol from the gas-phase studies at the B3LYP/6-311+G(d,p) level. Thus, while the inclusion of entropy and temperature corrections will reduce this dissociation energy, the complex **2__Te(OH)(NO_2)** is expected to be stable relative to the most favorable **2__Te(O)** + HONO dissociation limit by a few kilocalories/mole.

III.2. Comparison of the Mechanisms of the Reaction of 2__M + HOONO for M = Se and Te. The overall PESs of the reaction of **2__M** + HOONO for M = Se (previously reported[16]) and Te in the gas phase are presented in Figure 2. As this figure shows, the O^2-O^3 bond cleavage is a fast process for M = Se and Te. However, it is much faster for M = Te than for M = Se. Furthermore, the probability of competition in the concerted and stepwise pathways is higher for M = Te than for M = Se.

However, a noticeable difference in the mechanism of reaction 1 (M = Te) and reaction 2 (M = Se) comes from the comparison of the stability of the product complexes **2__M(OH)(ONO)**. For M = Se, this complex is less stable and easily dissociates to **2__Se(O)** + HONO and **2__Se(OH)•** + NO_2•. The formation of **2__Se(O)** and HONO is the more favorable channel and occurs with only 9.5 (3.7) kcal/mol energy loss, in the gas phase. On the contrary, for M = Te, the product **2__M(OH)(ONO)** is thermodynamically more stable than **2__Te(OH)•** + NO_2• and **2__Te(O)** + HONO dissociation limits by 23.7 (11.4) and 26.4 (14.5) kcal/mol kcal/mol, respectively. Thus, its dissociation to the **2__Te(OH)•** and NO_2• radicals is the most favorable channel in the gas phase. The inclusion of solvent effects makes the **2__Te(O)** formation process more favorable. In summary, *the reactions of **2__Se** and **2__Te** with HOONO proceed very fast. However, the reaction of **2__Se** with HOONO produces only the selenoxide **2__Se(O)**, while the reaction of **2__Te** with HOONO leads to the intermediate **2__Te(OH)(ONO)**, which is a few kilocalories/mole more stable relative to the most favorable dissociation limit of **2__Te(O)** + HONO.*

III.3. Comparison of the Mechanisms of the Reaction of 2__Te with PN and HOONO. Now, let us compare the mechanisms of the reactions of **2__Te** with $ONOO^-$ and HOONO.

Previously,[17] we have studied the mechanism of the reaction of **2__Te** + $ONOO^-$ and found that it proceeds via the formation of **2__Te(ONOO$^-$)** complex with 39.9 (28.9) kcal/mol complexation energy followed by 10.7 (10.1) kcal/mol O−O bond cleavage barrier resulting in the **2__Te(O)(NO_2^-)** product. *More importantly, the transition state corresponding to the O−O bond cleavage lies about 29.2 (18.7) kcal/mol lower than the reactants, indicating that the O−O activation process should occur extremely fast in the gas phase.* The rate-determining steps of the entire reaction are NO_2^- dissociation leading to **2__Te(O)** + **NO_2^-**, and NO_3^- formation via the transition state **2__Te-TS2**. Both processes start from the same **2__Te(O)(NO_2^-)** complex and occur by 36.6 (25.9) and 26.6 (26.9) kcal/mol energy loss, respectively. Since the NO_3^- formation barrier at **2__Te-TS2** is only (1.0) kcal/mol higher than the NO_2^- dissociation energy, we predict that nitrate formation will effectively compete with the NO_2^- dissociation during the reaction of **2__Te** with PN in the gas phase. The inclusion of solvent effects makes the reaction of **2__Te** + PN more facile and stabilizes the NO_2^- dissociation pathway over the nitrate formation one, and consequently makes the peroxynitrite → nitrate isomerization practically impossible. In water, the **2__Te(O)(NO_2^-)** → **2__Te(O)** + **NO_2^-** dissociation energy is calculated to be only 9.0 kcal/mol, not including entropy and temperature effects. The inclusion of these effects (estimated to be 12.2 kcal/mol from the gas-phase studies at the B3LYP/6-311+G(d,p) level) will, most probably, make the complex **2__Te(O)(NO_2^-)** less stable relative to the dissociation limit of **2__Te(O)** + **NO_2^-**.

Similarly, in the gas phase, the rate-determining step of the reaction of **2__Te** with HOONO is either the **2__Te(OH)•** + NO_2• or the **2__TeO** + HONO dissociation starting from the complex **2__Te(OH)(ONO)**, which occur with 23.7(11.4) and 26.4 (14.5) kcal/mol energy loss, respectively. Although the inclusion of solvent effects makes the **2__Te(O)** + HONO formation channel more favorable than **2__Te(OH)•** + NO_2•, the complex **2__Te(OH)(NO_2)** may still exist in the potential energy surface: in water, its dissociation to the most favorable products, **2__Te(O)** + HONO, is calculated to be 17.5 kcal/mol, without including entropy and temperature effects. The inclusion of these effects (which are estimated to be 11.4 kcal/mol from the gas-phase studies at the B3LYP/6-311+G(d,p) level) will reduce this dissociation energy, and the complex **2__Te(OH)(NO_2)** is expected to be stable to the most favorable **2__Te(O)** + HONO dissociation limit.

Thus, reaction of **2__Te** with $ONOO^-$ occurs very fast and leads to **2__Te(O)** and **NO_2^-** in solution. Although the reaction of **2__Te** with HOONO is also fast, it leads to the **2__Te(OH)(ONO)** complex and **2__Te(O)** + HONO products. Therefore, it is expected that telluroxide **2__Te(O)**, along with the complex **2__Te(OH)(ONO)**, could be involved in the reduction process by thiols (GPx activities of **2__Te**), which will be reported elsewhere.

IV. Conclusions

From the above discussion we may draw the following conclusions:

(1) In the gas phase, reaction of **2__Te** with HOONO proceeds via the concerted pathway with only a $\Delta H = 0.3$ kcal/mol HO−ONO bond cleavage barrier, calculated from the pre-reaction complex **2__Te(HOONO)**. However, the inclusion of entropy corrections (ΔG values) makes the concerted HO−ONO bond cleavage barrier (3.4) kcal/mol, which is larger than the (2.2) kcal/mol required for the HO−ONO bond homolysis, calculated at the B3LYP/BS1 level. Thus, in the gas phase, the stepwise pathway is more favorable than (or comparable to) the concerted one, after including entropy corrections. Inclusion of the solvent effects at the single-point PCM level increases the HO−ONO activation barrier to 5.8 kcal/mol, calculated from the reactants.

(2) The product of the HO−ONO bond cleavage by **2__Te** is the complex **2__Te(OH)(ONO)**, which could decay via two distinct pathways leading to NO_2• + **2__Te(OH)•** and **2__Te(O)** + HONO products. Both processes are endothermic (23.7 (11.4) and 26.4 (14.5) kcal/mol, respectively) in the gas phase. The inclusion of solvent effects stabilizes the **2__Te(O)** + HONO products more than NO_2• + **2__Te(OH)•**, and makes the former process more favorable in water. It is expected (even in water) that the final products of the reaction of **2__Te** + HOONO will be **2__Te(OH)(NO_2)** intermediate and **2__TeO** and HONO molecules.

(3) The comparison of the PES's of the reaction **2_M** + HOONO for M = Se (reported earlier[16]) and Te shows that the HO−ONO bond cleavage is fast for both M = Se and Te: the calculated HO−ONO bond cleavage barrier is smaller for M = Te than for M = Se. The probability of competition between the concerted and stepwise pathways is higher for M = Te than for M = Se. The reaction of **2__Se** with HOONO produces only selenoxide **2__Se(O)**, while the reaction of **2__Te** with HOONO may produce the intermediate **2__Te(OH)(ONO)** and **2__Te(O)** + HONO.

(4) Comparison of the PES's of the reactions **2__Te** + $ONOO^-$ (previously reported[17]) and **2__Te** + HOONO shows that both reactions are fast. The reaction of **2__Te** with $ONOO^-$ leads to the **2__Te(O)** and **NO_2^-** products, while the reaction of **2__Te** with HOONO leads to the **2__Te(OH)(ONO)** complex and **2__Te(O)** + HONO products. Therefore, telluroxide **2__Te(O)**, along with the **2__Te(OH)(ONO)** complex, is expected to be involved in the reduction by thiols (GPx activities of **2__Te**), which will be reported elsewhere.

Acknowledgment. Acknowledgment is made to the Cherry L. Emerson Center of Emory University for use of its resources, which is in part supported by a National Science Foundation grant (CHE-0079627) and an IBM Shared University Research

Award. D.G.M. thanks to National Science Foundation of the U.S.A. for financial support (CHE-0209660).

Supporting Information Available: Tables 1S and 2S showing geometries and bond energies of M_2 and MO molecules (M = S, Se, and Te) calculated at the various levels of theory; and Cartesian coordinates of all calculated reactants, intermediates, transition states, and products of the reaction **2_Te** + HOONO (Table 3S) and their total energies (Table 4S). This material is available free of charge via the Internet at http://pubs.acs.org.

References and Notes

(1) See: (a) Beckman, J. S.; Beckman, T. W.; Chen, J.; Marshall, P. A.; Freeman, B. A. *Proc. Natl. Acad. Sci. U.S.A.* **1990**, *87*, 1620. (b) Beckman, J. S.; Crow, J. P. *Biochem. Soc. Transact.* **1993**, *21*, 330. (c) Ischiropoulos, H.; Zhu, L.; Beckman, J. S. *Arch. Biochem. Biophys.* **1992**, *298*, 446. (d) Huie, R. E.; Padmaja, S. *Free Radical Res. Commun.* **1993**, *18*, 195.

(2) Kissner, R.; Koppenol, W. H. *J. Am. Chem. Soc.* **2002**, *124*, 234 and references therein.

(3) Pryor, W. A.; Gueto, R.; Jin, X.; Koppenol, W. H.; Ngu-Schwemlein, M.; Squadrito, G. L.; Uppu, P. L.; Uppu, R. M. *Free Radical Biol. Med.* **1995**, *18*, 75.

(4) The term peroxynitrite is used to refer to the peroxynitrite anion O═NOO⁻, and peroxynitrous acid, HOONO, unless otherwise indicated. The IUPAC recommended names are oxoperoxonitrate(−1) and hydrogen oxoperoxonitrate, respectively. In this paper, the abbreviation PN is used to refer to the peroxynitrite anion O═NOO⁻.

(5) (a) Halliwell, B.; Zhao, K.; Whiteman, M. *Free Radical Res.* **1999**, *31*, 651. (b) Pfeiffer, S.; Mayer, B.; Hemmens, B. *Angew. Chem., Int. Ed.* **1999**, *38*, 1715. (c) Groves, J. T. *Curr. Opin. Chem. Biol.* **1999**, *3*, 226. (d) Hurst, J. K.; Lymar, S. V. *Acc. Chem. Res.* **1999**, *32*, 520. (e) Trujillo, M.; Navillat, M.; Alvarez, M. N.; Peluffo, P.; Radi, R. *Analusis* **2000**, *28*, 518. (f) Radi, R.; Peluffo, P.; Alvarez, M. N.; Naviliat, M.; Cayota, A. *Free Radical Biol. Med.* **2001**, *30*, 463.

(6) (a) *Selenium in Biology and Human Health*; Burk, R. F., Ed.; Springer-Verlag: New York, 1994, and references therein. (b) Epp, O.; Ladenstein, R.; Wendel, A. *Eur. J. Biochem.* **1983**, *133*, 51. (c) Ren, B.; Huang, W.; Akesson, B.; Ladenstein, R. *J. Mol. Biol.* **1997**, *268*, 869.

(7) (a) Mugesh, G.; Singh, H. B. *Chem. Soc. Rev.* **2000**, *29*, 347. (b) Mugesh, G.; Panda, A.; Singh, H. B.; Punekar, N. S.; Butcher, R. J. *J. Am. Chem. Soc.* **2001**, *123*, 839. (c) Mugesh, G.; du Mont W. W.; Sies, H. *Chem. Rev.* **2001**, *101*, 2125 and references therein. (d) Briviba, K.; Roussyn, I.; Sharov, V. S.; Sies, H. *Biochem. J.* **1996**, *319*, 13.

(8) (a) Mugesh, G.; du Mont W. W.; Sies, H. *Chem. Rev.* **2001**, *101*, 2125 and references therein. (b) Briviba, K.; Roussyn, I.; Sharov, V. S.; Sies, H. *Biochem. J.* **1996**, *319*, 13. (c) Sies, H.; Masumoto, H. *Adv. Pharmacol.* **1997**, *38*, 229 and references therein.

(9) Back, T. G.; Moussa, Z. *J. Am. Chem. Soc.* **2002**, *124*, 12104.

(10) Jacob, C.; Arteel, G. E.; Kanda, T.; Engman, L.; Sies, H. *Chem. Res. Toxicol.* **2000**, *13*, 3 and references therein.

(11) Mugesh, G.; Panda, A.; Kumar, S.; Apte, S. D.; Singh, H. B.; Butcher, R. J. *Organometallics* **2002**, *21*, 884 and references therein.

(12) (a) Ren, X.; Xue, Y.; Liu, J.; Zhang, K.; Zheng, J.; Luo, G.; Guo, C.; Mu, Y.; Shen, J. *ChemBioChem* **2002**, *3*, 356. (b) Ren, X.; Xue, Y.; Zhang, K.; Liu, J.; Luo, G.; Zheng, J.; Mu, Y.; Shen, J. *FEBS Lett.* **2001**, *507*, 377.

(13) (a) Engman, L.; Stern, D.; Pelcman, M.; Anderson, C.-M. *J. Org. Chem.* **1994**, *59*, 1973. (b) Engman, L.; Persson, J.; Vessman, K.; Ekstorm, M.; Berglund, M.; Anderson, C.-M. *Free Radical Biol. Med.* **1995**, *19*, 441. (c) Vessman, K.; Ekstorm, M.; Berglund, M.; Anderson, C.-M.; Engman, L. *J. Org. Chem.* **1995**, *60*, 4461. (d) Anderson, C.-M.; Hallberg, A.; Brattsand, R.; Cotgreave, I. A.; Engman, L.; Persson, J. *Bioorg. Med. Chem. Lett.* **1993**, *3*, 2553. (e) Anderson, C.-M.; Brattsand, R.; Hallberg, A.; Engman, L.; Persson, J.; Moldeus, P.; Cotgreave, I. A. *Free Radical Res.* **1994**, *20*, 401. (f) Wieslander, E.; Engman, L.; Svensjo, E.; Erlansson, M.; Johansson, U.; Linden, M.; Anderson, C.-M.; Brattsand, R. *Biochem. Pharmacol.* **1998**, *55*, 573. (g) Briviba, K.; Tamler, R.; Klotz, L.-O.; Engman, L.; Cotgreave, I. A.; Sues, H. *Biochem. Pharmacol.* **1998**, *55*, 817. (h) Kanda, T.; Engman, L.; Cotgreave, I. A.; Powis, G. *J. Org. Chem.* **1999**, *64*, 8161.

(14) You, Y.; Ahsan, K.; Detty, M. R. *J. Am. Chem. Soc.* **2003**, *125*, 4918 and references therein.

(15) Musaev, D. G.; Geletii, Y. A.; Hill, G.; Hirao, K. *J. Am. Chem. Soc.* **2003**, *125*, 3877.

(16) Musaev, D. G.; Hirao, K. *J. Phys. Chem.* A **2003**, *107*, 1563.

(17) Sakimoto, Y.; Hirao, K.; Musaev, D. G. *J. Phys. Chem.* A **2003**, *107*, 5631.

(18) (a) Pryor, W. A.; Jin. X.; Squadrito, G. J. *Proc. Natl. Acad. Sci. U.S.A.* **1994**, *91*, 11173. (b) Jensen, J. L.; Miller, B. L.; Zhang, X.; Hug, G. L.; Schoeneich, C. *J. Am. Chem. Soc.* **1997**, *119*, 4749.

(19) (a) Miertus, S.; Scrocco, E.; Tomasi, J. *Chem. Phys.* **1981**, *55*, 117. (b) Miertus, S.; Tomasi, J. *Chem. Phys.* **1982**, *65*, 239. (c) Cossi, M.; Barone, V.; Cammi, R.; Tomasi, J. *Chem. Phys. Lett.* **1996**, *255*, 327. (d) Cances, M. T.; Mennucci, V.; Tomasi, J. *J. Chem. Phys.* **1997**, *107*, 3032. (e) Barone, V.; Cossi, M.; Tomasi, J. *J. Comput. Chem.* **1998**, *19*, 404.

(20) (a) Houk, K. N.; Condroski, K. R.; Pryor, W. A. *J. Am. Chem. Soc.* **1996**, *118*, 13002. (b) Houk, K. N.; Liu, J.; DeMello, N. C.; Condorski, K. R. *J. Am. Chem. Soc.* **1997**, *119*, 10147. (c) Yang, D.; Tang, Y. C.; Chen, J.; Wang, X. C.; Bartberger, M. D.; Houk, K. N.; Olson, L. *J. Am. Chem. Soc.* **1999**, *121*, 11976. (d) Bartberger, M. D.; Olson, L. P.; Houk, K. N. *Chem Res. Toxicol.* **1998**, *11*, 710 and references therein.

(21) Bach, R. D.; Gluhkovtsev, M. N.; Canepa, C. *J. Am. Chem. Soc.* **1998**, *120*, 775.

(22) Shustov, G. V.; Spinney, R.; Rauk, A. *J. Am. Chem. Soc.* **2000**, *122*, 1191.

(23) Musaev, D. G.; Geletii, Y. A.; Hill, G. *J. Phys. Chem.* A **2003**, *107*, 5862.

(24) Frisch, M. J.; Trucks, G. W.; Schlegel, H. B.; Scuseria, G. E.; Robb, M. A.; Cheeseman, J. R.; Zakrzewski, V. G.; Montgomery, J. A., Jr.; Stratmann, R. E.; Burant, J. C.; Dapprich, S.; Millam, J. M.; Daniels, A. D.; Kudin, K. N.; Strain, M. C.; Farkas, O.; Tomasi, J.; Barone, V.; Cossi, M.; Cammi, R.; Mennucci, B.; Pomelli, C.; Adamo, C.; Clifford, S.; Ochterski, J.; Petersson, G. A.; Ayala, P. Y.; Cui, Q.; Morokuma, K.; Malick, D. K.; Rabuck, A. D.; Raghavachari, K.; Foresman, J. B.; Cioslowski, J.; Ortiz, J. V.; Baboul, A. G.; Stefanov, B. B.; Liu, G.; Liashenko, A.; Piskorz, P.; Komaromi, I.; Gomperts, R.; Martin, R. L.; Fox, D. J.; Keith, T.; Al-Laham, M. A.; Peng, C. Y.; Nanayakkara, A.; Gonzalez, C.; Challacombe, M.; Gill, P. M. W.; Johnson, B.; Chen, W.; Wong, M. W.; Andres, J. L.; Gonzalez, C.; Head-Gordon, M.; Replogle, E. S.; Pople, J. A. *Gaussian 98*, Revision A.7;Gaussian, Inc.: Pittsburgh, PA, 1998.

(25) (a) Becke, A. D. *Phys. Rev. A* **1988**, *38*, 3098. (b) Lee, C.; Yang, W.; Parr, R. G. *Phys. Rev. B* **1988**, *37*, 785. (c) Becke, A. D. *J. Chem. Phys.* **1993**, *98*, 5648.

(26) Dolg, M.; Wedig, U.; Soll, H.; Preuss, H. *J. Chem. Phys.* **1987**, *86*, 866.

(27) *CRC Handbook of Chemistry and Physics*, 72nd ed.; Lide, D. R., Ed.; CRC Press: Boca Raton, FL, 1991−1992.

(28) See refs 15, 16, 17, 18, and references therein.

(29) Lynch, B. J.; Fast, P. L.; Harris, M.; Truhlar, D. G. *J. Phys. Chem.* A **2000**, *104*, 4811.

(30) Cossi, M.; Adamo, C.; Barone, V. *Chem. Phys. Lett.* **1998**, *297*, 1.

(31) See refs15, 16, 17, and references therein.

(32) McGrath, M. P.; Rowland, F. S. *J. Chem. Phys.* **1994**, *98*, 1061 and references therein.

(33) (a) Gonzalez, C.; Schlegel, H. B. *J. Chem. Phys.* **1989**, *90*, 2154. (b) Gonzalez, C.; Schlegel, H. B. *J. Phys. Chem.* **1990**, *94*, 5523.

(34) (a) Sumathi, R.; Peyerimhoff, S. D. *J. Chem. Phys.* **1997**, *107*, 1872, (b) Bach, R. D.; Ayala, P. Y.; Schelegel, H. B. *J. Am. Chem. Soc.* **1996**, *118*, 12758.

(35) Pfeiffer, S.; Mayer, B.; Janoschek, R. *THEOCHEM* **2003**, *623*, 95.

(36) Koppenol, W. H.; Moreno, J. J.; Pryor, W. A.; Ischiropoulos, H.; Beckman, J. S. *Chem. Res. Toxicol.* **1992**, *5*, 834.